

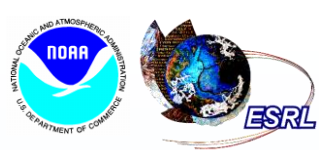
OCEAN SURFACE ROUGHNESS REFLECTOMETRY WITH GPS MULTISTATIC RADAR FROM HIGH-ALTITUDE AIRCRAFT

VALERY U. ZAVOROTNY¹, DENNIS M. AKOS², HANNA MUNTZING³

¹NOAA/Earth System Research Laboratory/
Physical Sciences Division, USA

²University of Colorado at Boulder/
Aerospace Engineering Sciences, USA

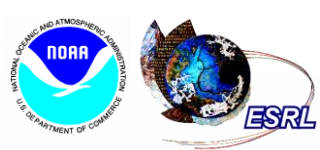
³Luleå University of Technology, Sweden



Outline



- **2010 NOAA G-IV experiment and data collection**
- **Data analysis**
- **Wind retrievals and comparisons**
- **A role of the waveform Doppler filtering in wind retrievals**
- **Conclusions**



2010 North Pacific high-altitude experiment



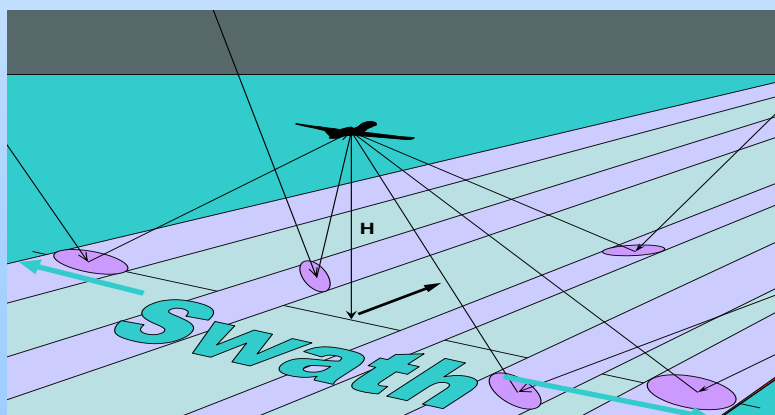
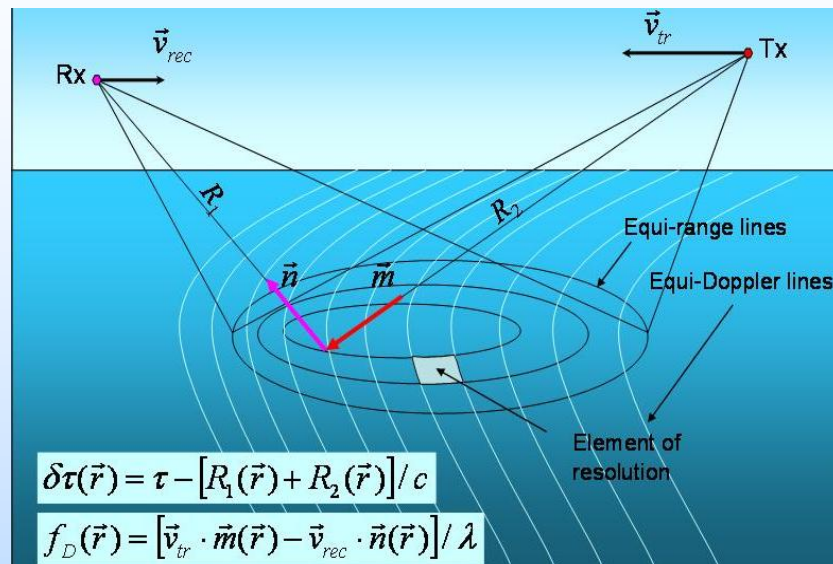
A modified version of the CU bistatic radar with a larger bandwidth front end was installed on the NOAA Gulfstream-IV jet aircraft and operated during flights in January, 2010 to test the system at higher altitudes, 13,000 m, which should give insight into the feasibility of using this technique for high-altitude UAS platforms.

The flight track ran across the Northern Pacific Ocean and the GPS reflected signal was recorded from all available satellites. Overall, more than 20 hours of reflection data were obtained during three flights. Wind speed and direction from dropsondes deployed from the same aircraft were available to assess the capability of this multistatic GPS radar to monitor winds or ocean surface roughness.

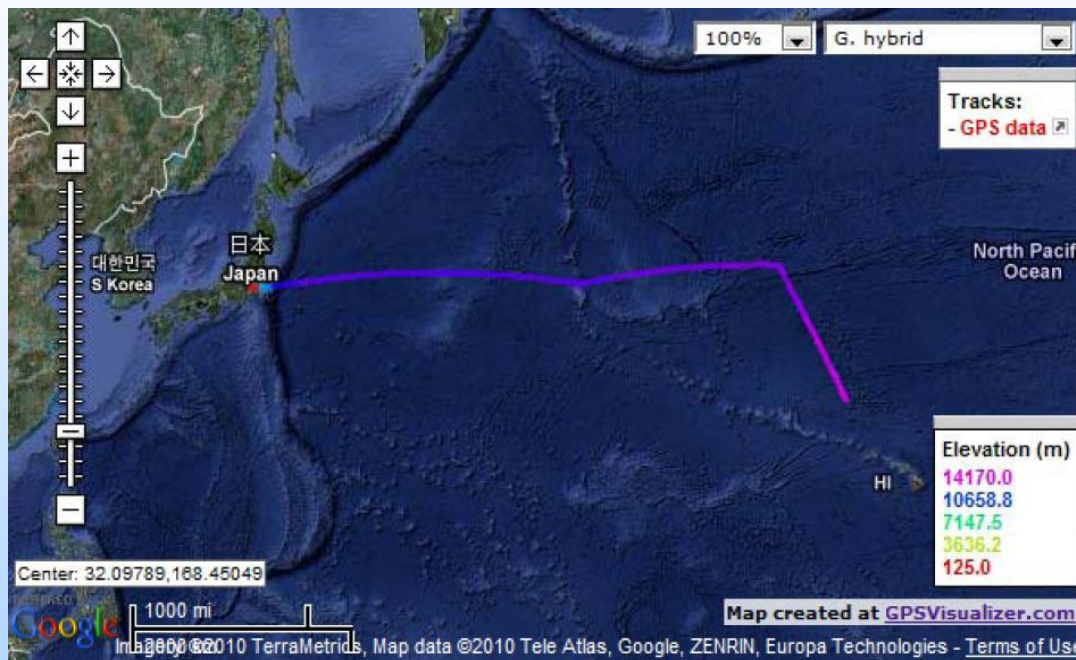
Only a small part of the raw data is processed at this point. Here we present a segment of the processed data from flight #3 on Jan. 24 and comparisons with reflected waveform calculations based on our theoretical model.

2010 North Pacific high-altitude experiment: platform and scattering geometry

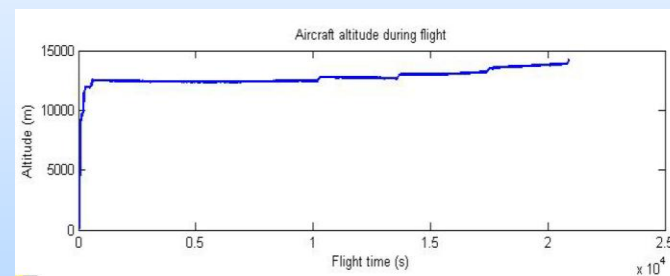
NOAA Gulfstream IV jet



G-IV flight track on January 24, 2010



Flight #3
Start: 08:09 UTC
Stop: 14:34 UTC
Duration: 6 h 25 m
Data volume: 370 GB

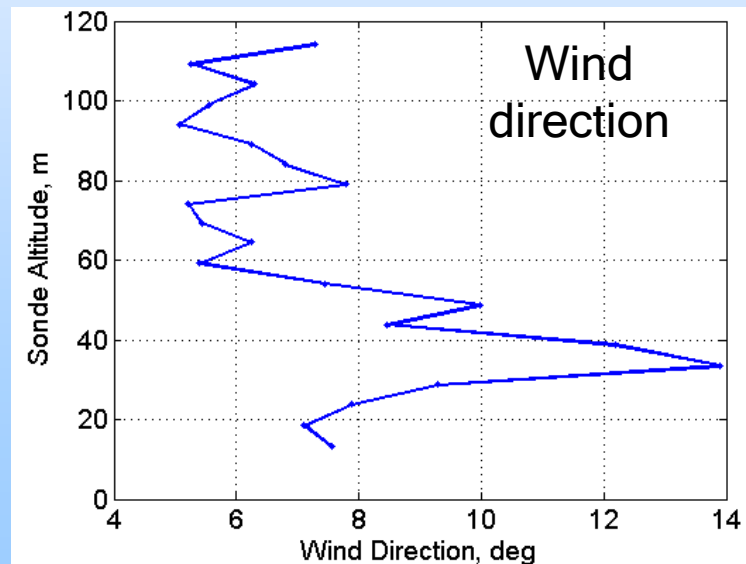
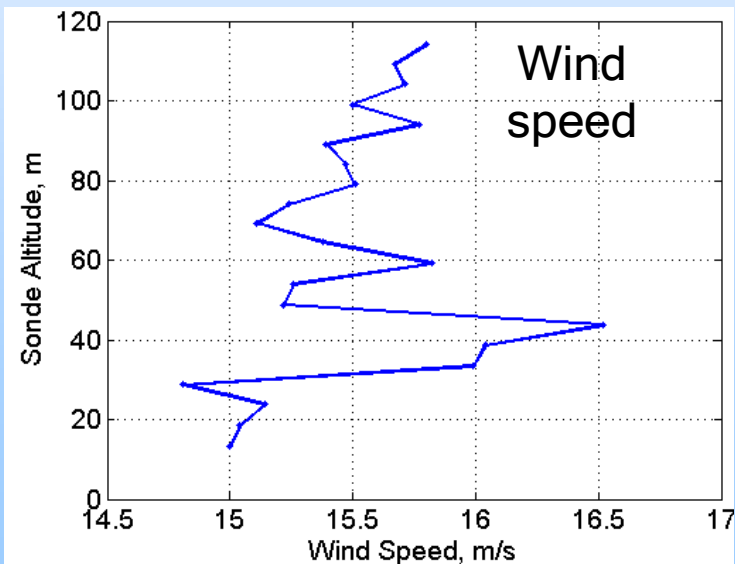
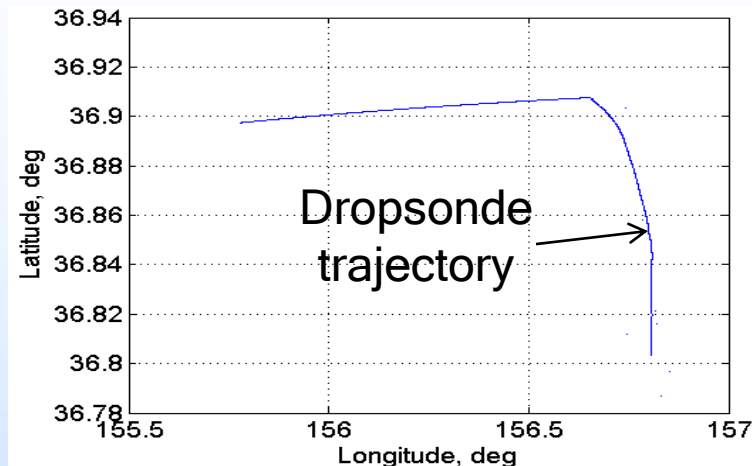


Wind speed and direction from GPS dropsondes deployed from the aircraft

Segment 1: 9:56 -10:16 UTC

Near-surface wind speed: 15 m/s

Near-surface wind direction: 7 deg

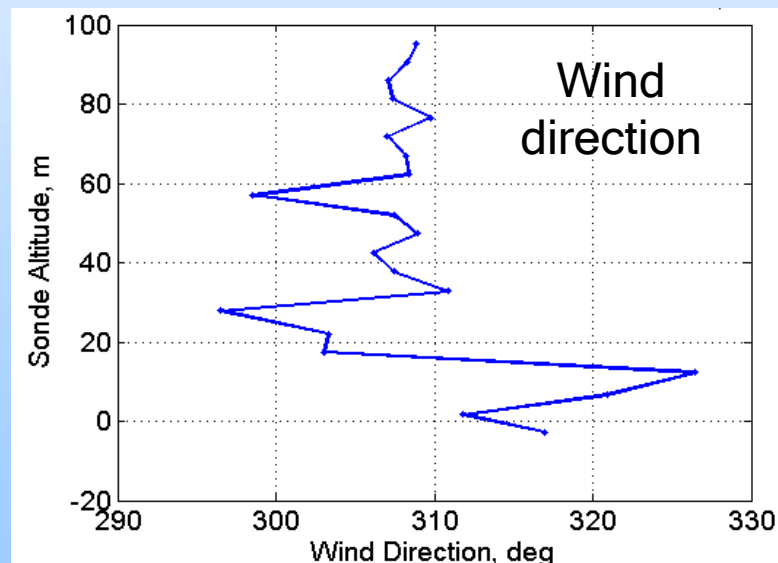
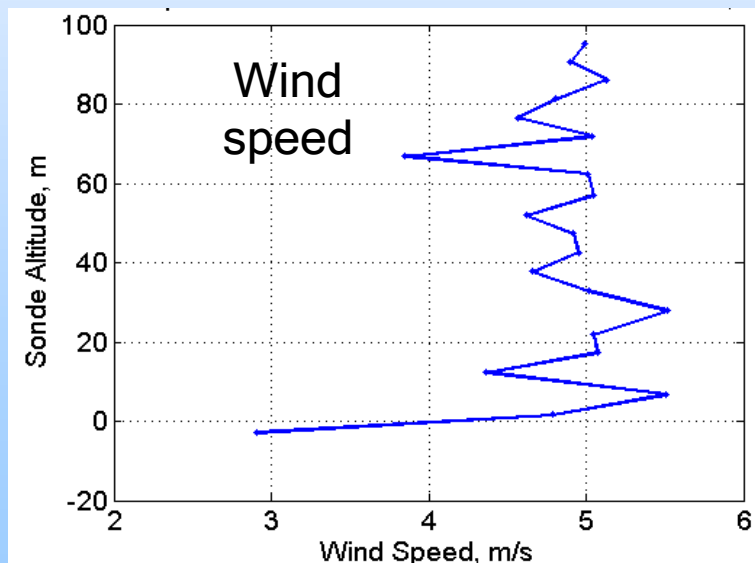
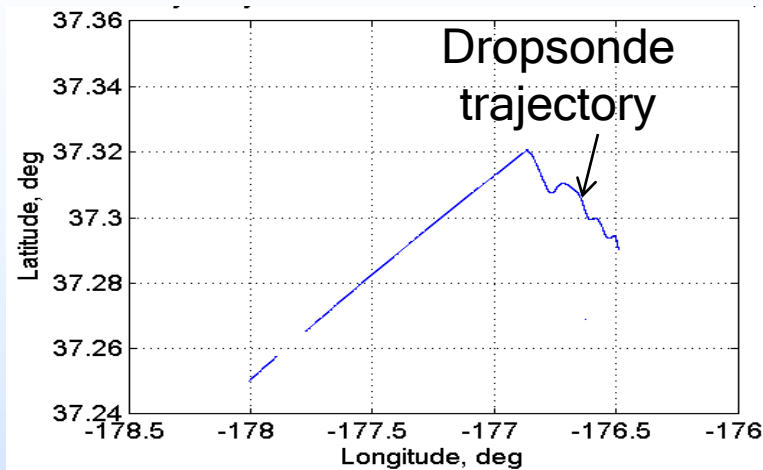


Wind speed and direction from GPS dropsondes deployed from the aircraft (cont'd)

Segment 2: 12:14 -12:36 UTC

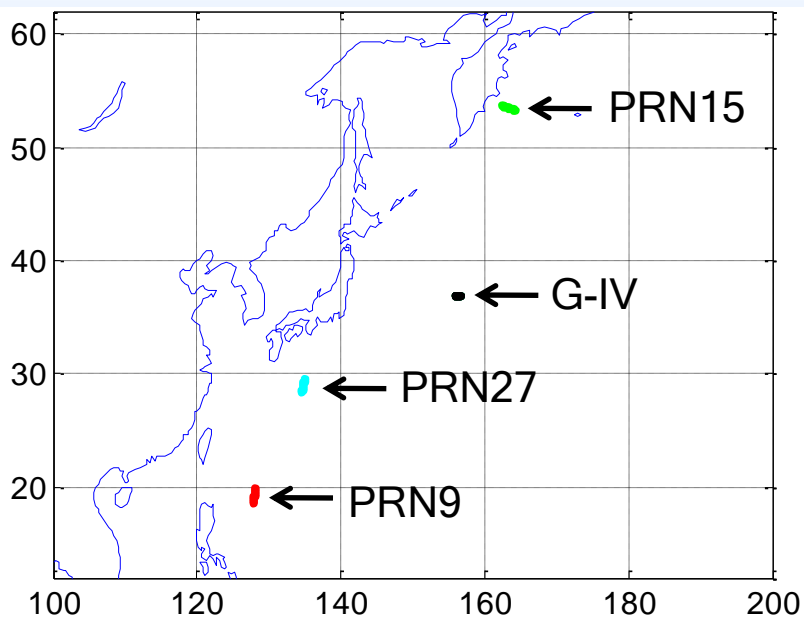
Near-surface wind speed: 5 m/s

Near-surface wind direction: 310 deg

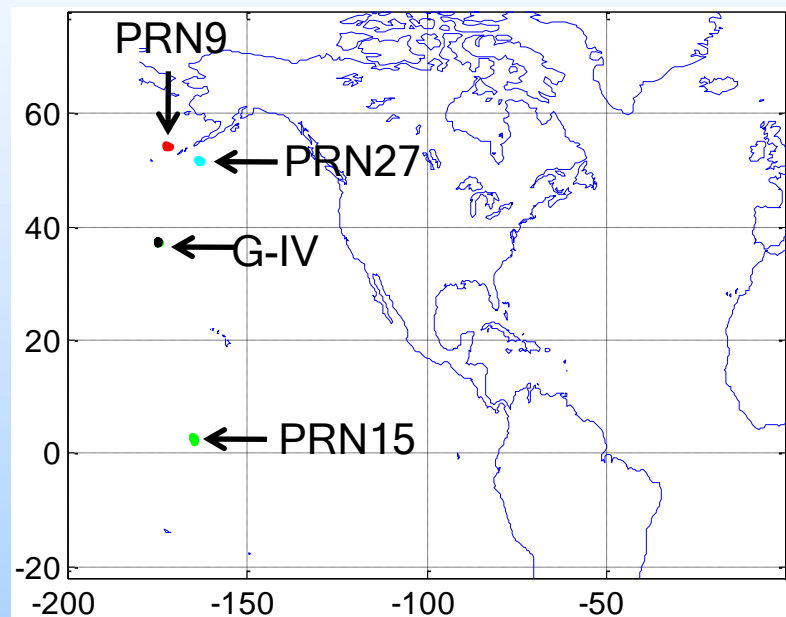


Ground tracks of GPS satellites and the G-IV aircraft

**10:00 UTC
(200 s)**

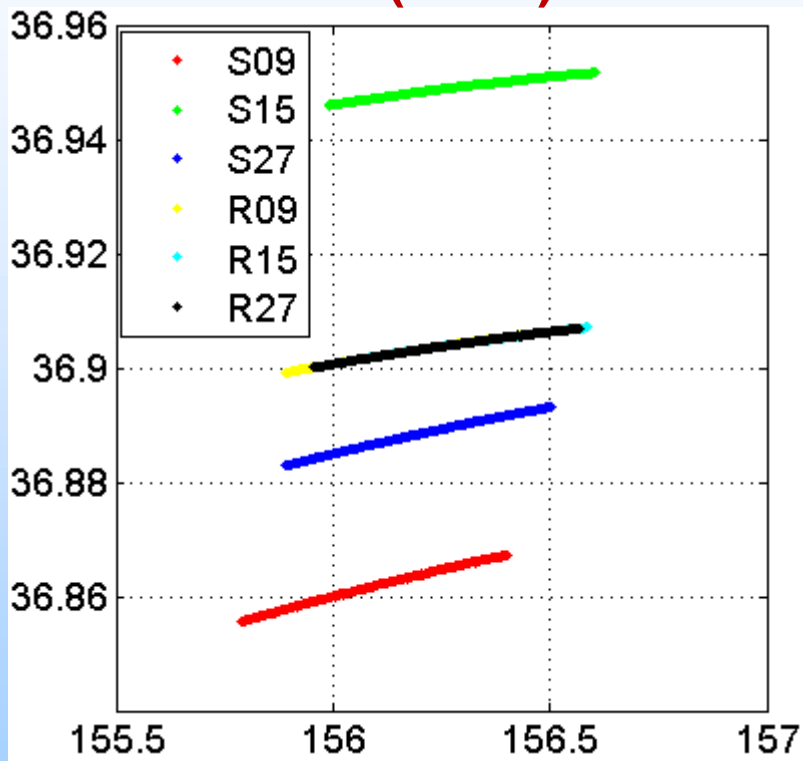


**12:30 UTC
(100 s)**

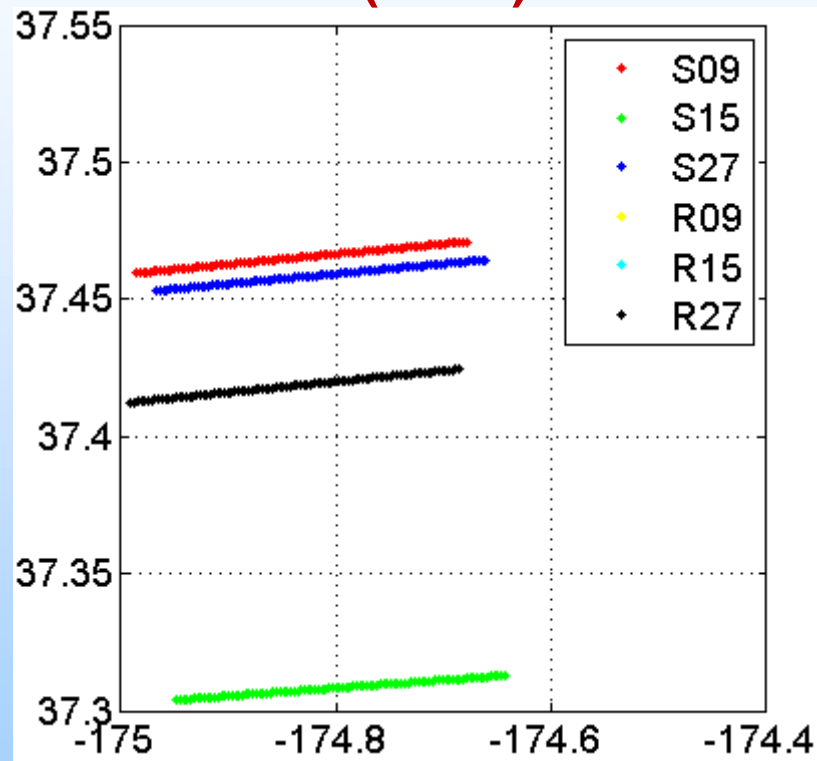


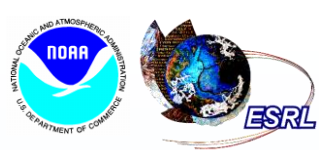
Ground tracks of GPS specular points and the G-IV aircraft

**10:00 UTC
(200 s)**



**12:30 UTC
(100 s)**





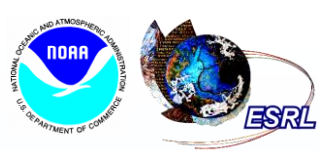
Log of segments with processed data

Satellite	Start time (UTC)	Stop time (UTC)	Az/EI (degrees)	Altitude (m)
PRN9	9:56:31	9:59:51	242/51	12359.804
	10:06:31	10:09:51	249/53	12356.99
	10:00:00	10:01:40	244/52	12361.401
	11:28:29	11:31:49	358/67	12684.547
	12:30:00	12:31:40	6/68	12680.054
PRN 15	9:56:59	10:01:19	14/68	12368.445
	10:06:59	10:01:19	22/69	12366.119
	10:00:00	10:01:40	16/68	12361.401
	12:22:54	12:26:14	160/48	12676.592
	12:30:00	12:31:40	163/45	12680.054
PRN 27	9:56:52	10:01:12	251/65	12368.168
	10:06:52	10:10:12	262/66	12364.679
	10:00:00	10:01:40	255/65	12361.401
	12:21:40	12:25:00	19/68	12684.71
	12:30:00	12:31:40	26/69	12680.054

Velocity components in the local Cartesian coordinates for both the aircraft and the satellite

Velocities, m/s: v , for aircraft u , for satellite	V_x	V_y	V_z	U_x	U_y	U_z
PRN9/1 segm.	125.62	-250.34	-0.33	-2048.03	-2150.81	1181.74
PRN9/2 segm.	-282.13	41.78	0.11	-2783.21	-818.96	266.99
PRN15/1 segm.	-270.40	72.35	0.03	-2763.89	-79.38	30.27
PRN15/2 segm.	276.50	69.94	0.22	-447.44	2540.45	-1838.36
PRN27/1 segm.	68.36	-269.83	-0.37	-2266.50	-1867.96	743.01
PRN27/2 segm.	-250.25	136.81	0.18	-2734.84	-163.80	22.55

These velocities were calculated from measured ECEF velocities. For each aircraft-satellite pair a right Cartesian xyz coordinate system was introduced with yz-plane crossing locations of the aircraft, the satellite, and the reflection point.



Waveform data processing



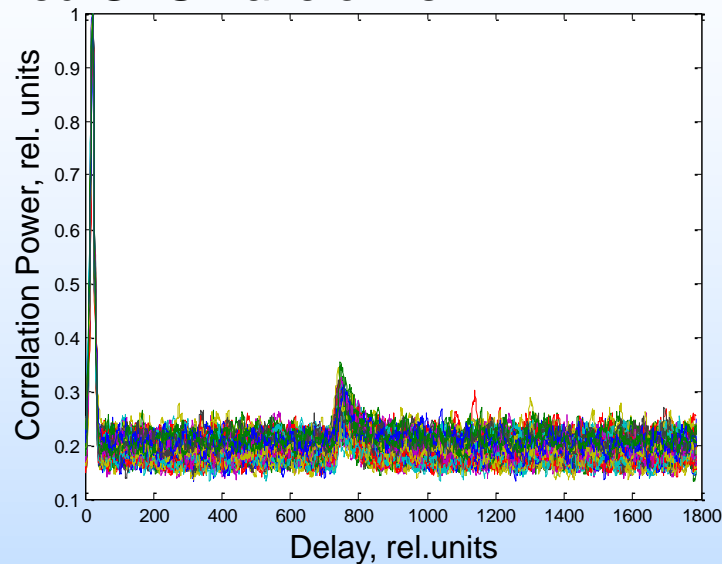
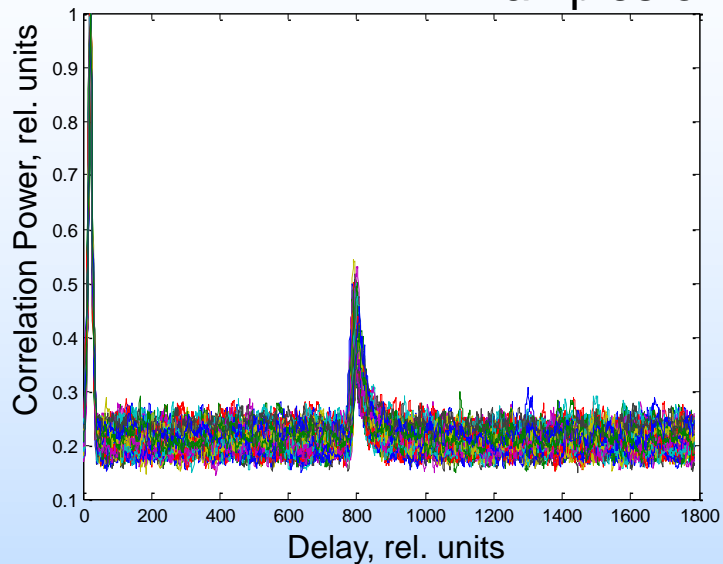
The cross-correlations between raw signals and the PRN codes of three chosen satellites were calculated over coherent integration time 1 ms, with an incoherent post-averaging of obtained waveforms over 200 ms.

A longer integration time is not feasible because migrating of the peak position would lead to the smearing of the waveforms.

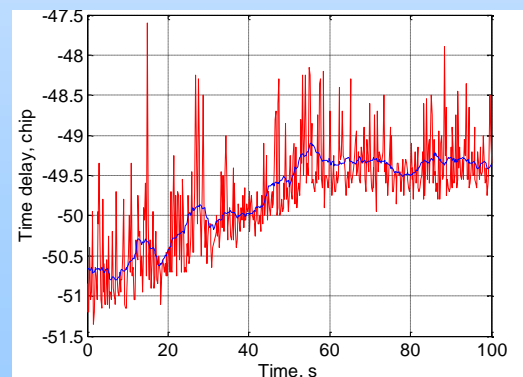
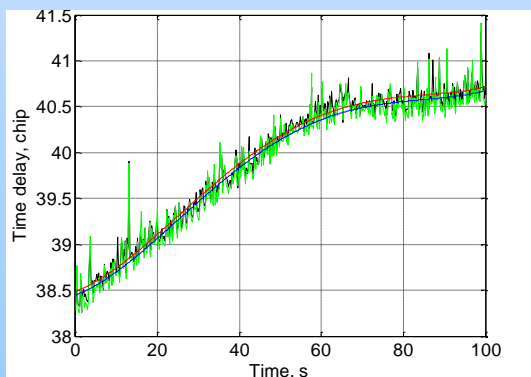
The following steps were taken during next levels of data processing:

1. Search for a peak position in each such realization.
2. Removal of the noise from the curve "peak position vs time" by interpolating it by a 5th-order polynomial.
3. Alignment of all waveforms for each PRN to a single peak position.
4. Calculation of the noise floor by averaging the noise from time offset intervals away from the reflected waveforms.
5. Subtraction of the noise floor from the waveforms and normalizing them by the peak value.
6. Additional averaging of the waveforms over 20 s which gives us 5 segments from 100-s total length of the data.

Examples of retrieved GPS waveforms



Examples of a delay between reflected and reflected GPS waveforms



Reflected waveform modeling

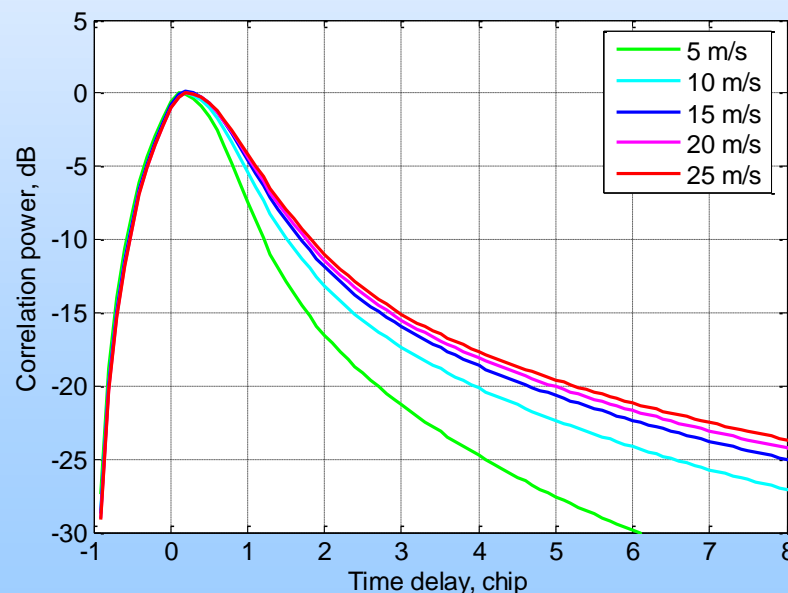
$$Y(t_0, \tau) = \int_0^{T_i} a(t_0 + t') u(t_0 + t' + \tau) \exp(2\pi i f_c t') dt'$$

$$\langle |Y(\tau)|^2 \rangle = \iint \frac{GA^2(\tau - (R_0 + R)/c) |S(f_D - f_c + f_0)|^2}{4R_0^2 R^2} \sigma_0 d^2\eta$$

$$\sigma_0 = \frac{|\mathfrak{R}|^2 q^4}{q_z^4} P\left(\vec{s} = -\frac{\vec{q}_\perp}{q_z}\right)$$

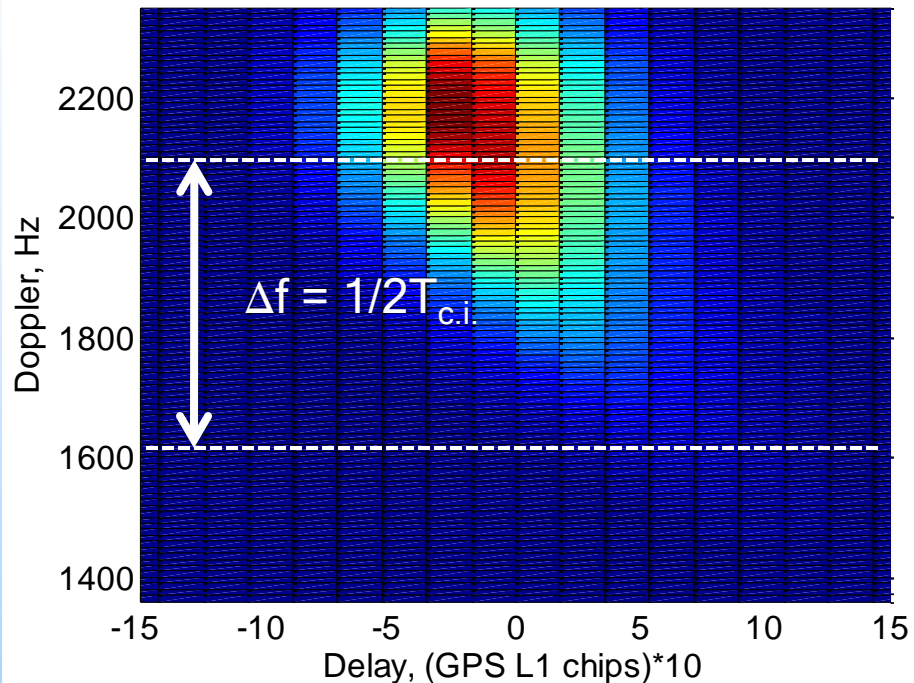
P is the Gaussian PDF of L-band limited slopes of the sea surface. Variances of slopes are calculated from the Elfouhaily spectrum. The width of the spectrum is proportional to the wind speed.

An example of modeled reflected waveforms without taking into account the Doppler filtering ($|S|^2=1$)



Effect of Doppler filtering on waveforms

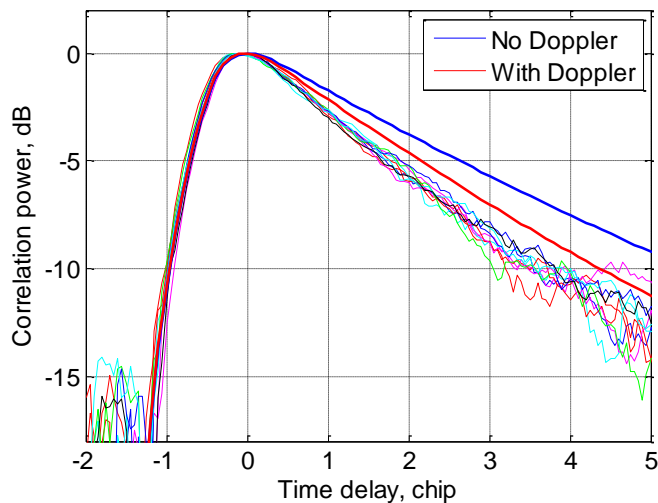
An example of the delay-Doppler map for PRN9, segment 1.



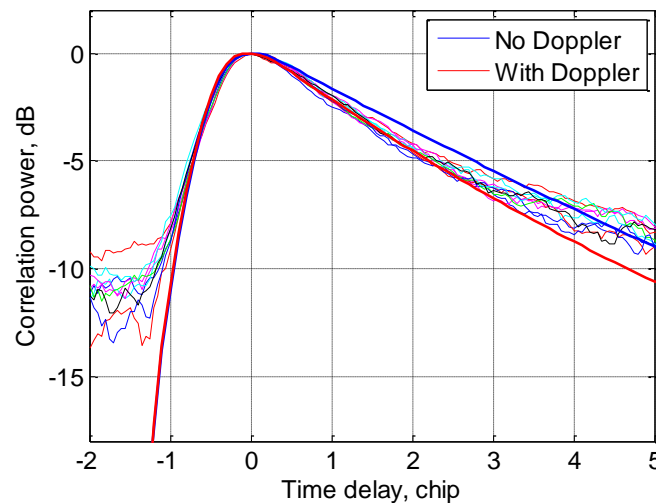
When the frequency offset is not optimal then the finite width of the Doppler filter $|S|^2$ can modify the shape of the waveform

Comparison between measured and modeled GPS reflected waveforms

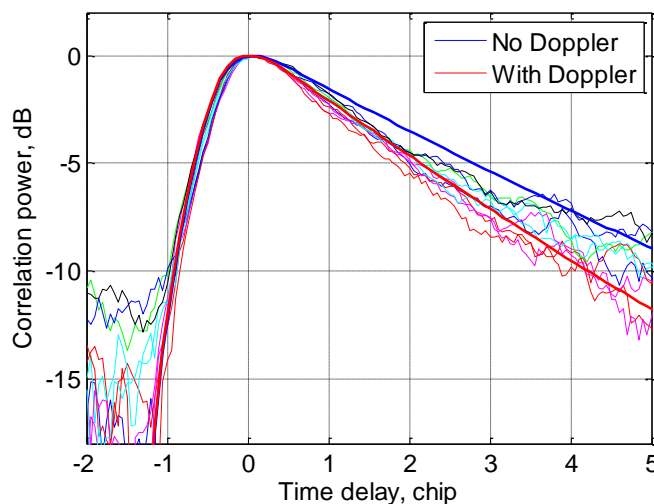
Waveforms for PRN#9 (9:56 UTC, $U_{10} = 15$ m/s)



Waveforms for PRN#15 (9:56 UTC, $U_{10} = 15$ m/s)



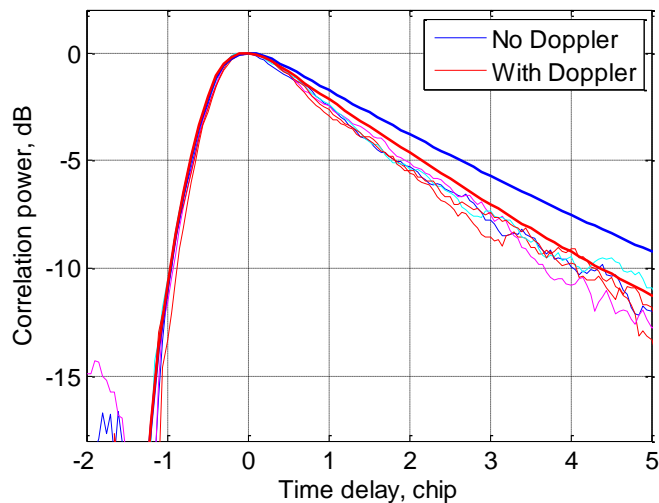
Waveforms for PRN#27 (9:56 UTC, $U_{10} = 15$ m/s)



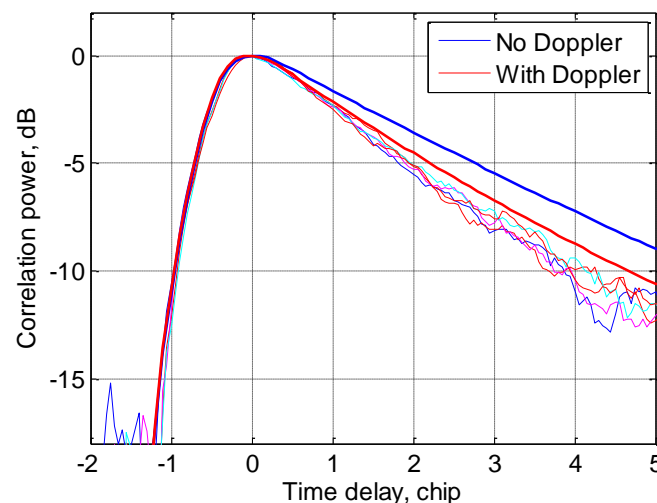
Segment 1a
 $U_{10} = 15$ m/s

Comparison between measured and modeled GPS reflected waveforms (con'd)

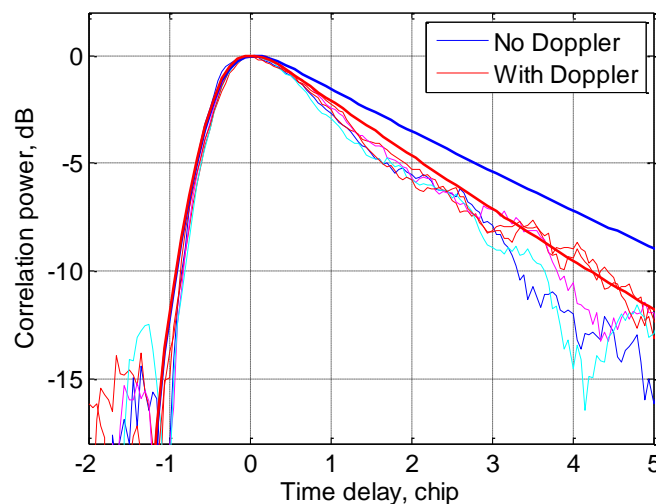
Waveforms for PRN#9 (10:00 UTC, $U_{10} = 15$ m/s)



Waveforms for PRN#15 (10:00 UTC, $U_{10} = 15$ m/s)



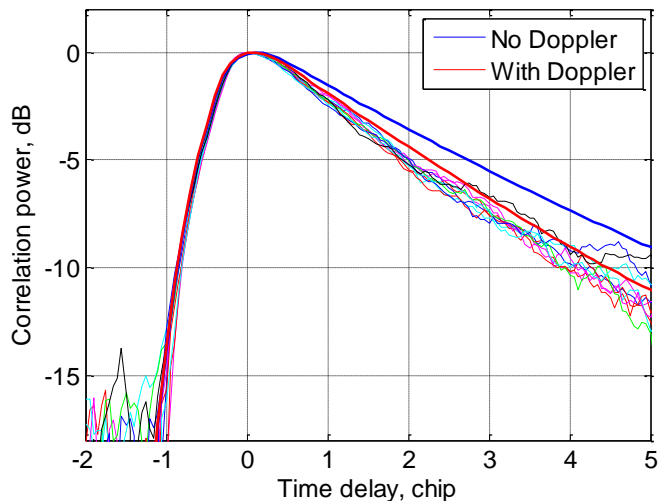
Waveforms for PRN#27 (10:00 UTC, $U_{10} = 15$ m/s)



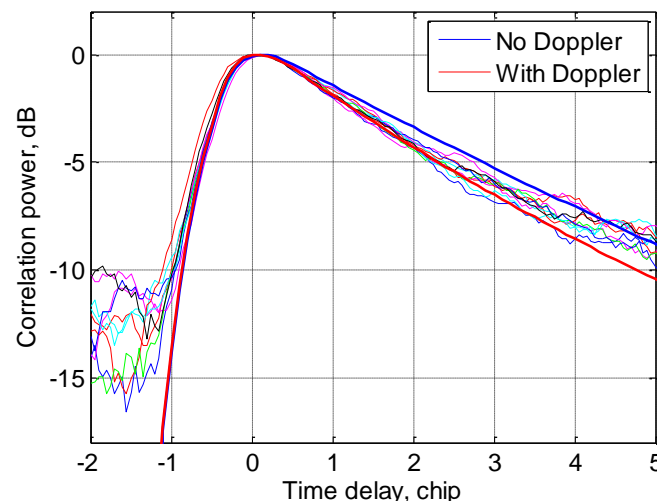
Segment 1b
 $U_{10} = 15$ m/s

Comparison between measured and modeled GPS reflected waveforms (con't)

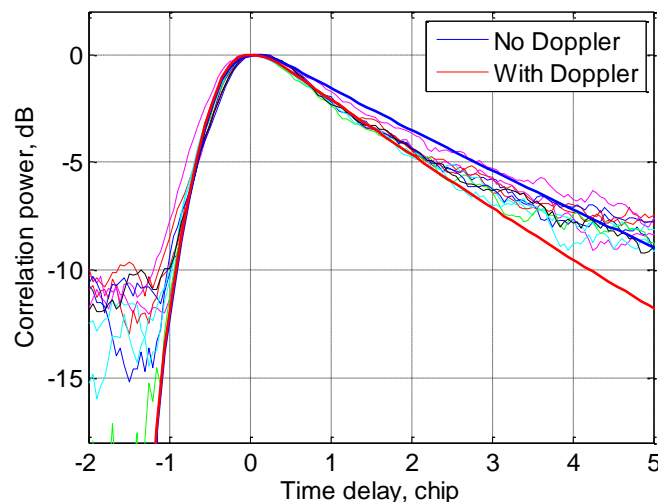
Waveforms for PRN#9 (10:06 UTC, $U_{10} = 15$ m/s)



Waveforms for PRN#15 (10:06 UTC, $U_{10} = 15$ m/s)



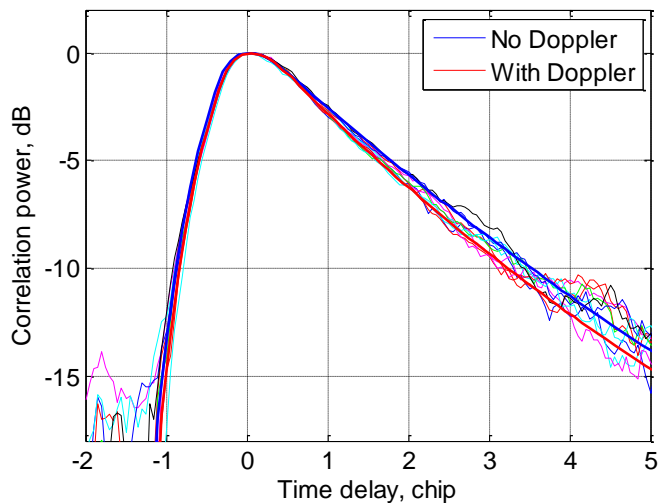
Waveforms for PRN#27 (10:06 UTC, $U_{10} = 15$ m/s)



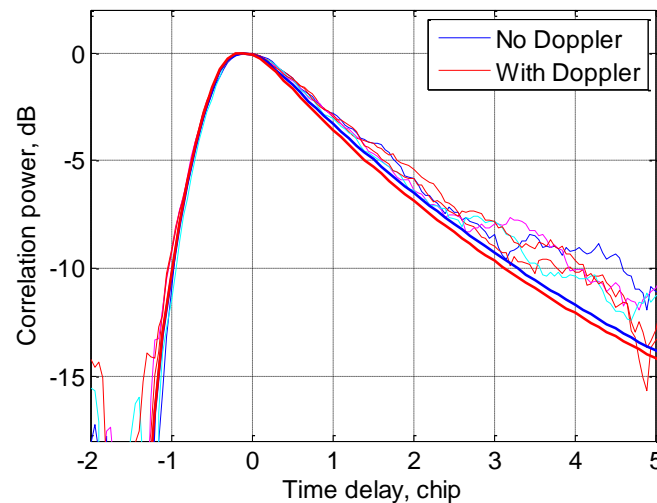
Segment 1c
 $U_{10} = 15$ m/s

Comparison between measured and modeled GPS reflected waveforms (con't)

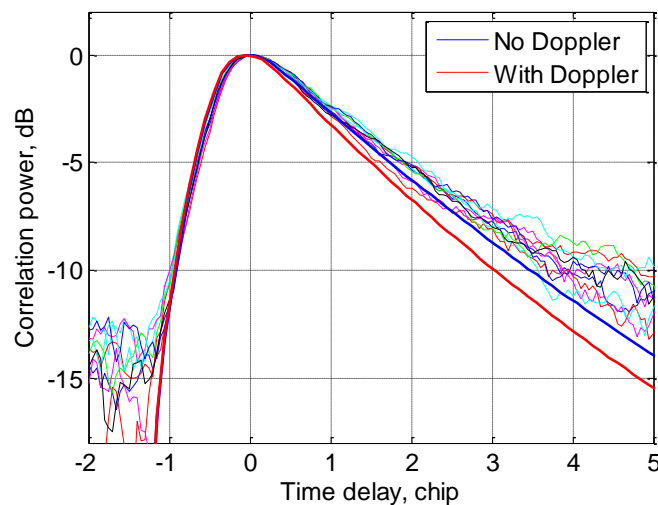
Waveforms for PRN#9 (12:30 UTC, $U_{10} = 5$ m/s)



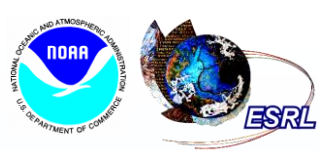
Waveforms for PRN#15 (12:30 UTC, $U_{10} = 5$ m/s)



Waveforms for PRN#27 (12:30 UTC, $U_{10} = 5$ m/s)



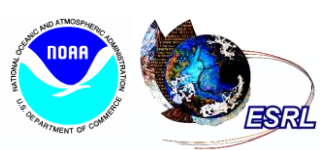
Segment 2
 $U_{10} = 5$ m/s



Conclusions



- The 2010 G-IV experiment was concerned with testing the software GPS bistatic radar under quiescent, uniform wind conditions from a high altitude aircraft.
- We presented first results from high-altitude experiments on GPS ocean reflections using CU multistatic GPS radar.
- Despite a limited data obtained the results of the experiment indicate that the GPS bistatic radar technique of surface wind measurement works well under conditions where an equilibrium between local wind and the surface waves exists and elevation angles higher than 30° .
- Comparisons with scattering modeling results show that the effect of Doppler filtering of the reflected waveforms due to a relatively high speed of the G-IV aircraft cannot be neglected and should be properly accounted when performing surface wind retrieval.
- Presented here results are very tentative and require more thorough analysis of the data, much further validation.



Many thanks to:

Chris Fairall, NOAA/ESRL/PSD3 Branch Chief, and
Robby Hood, NOAA UAS Program Director, for their
support of this project;

Ed Walsh, NOAA/ESRL, for fruitful discussions;

Terry Lynch,

Jeff Smith,

Jim Roles,

Mark Rogers,

Joe Greene,

of NOAA/Aircraft Operations Center, for their help with
installation and operation of the CU multistatic GPS radar.